Developmental Patterns Based Individualized Parcellation of Infant Cortical Surface

Gang Li(✉), Li Wang, Weili Lin, and Dinggang Shen

Department of Radiology and BRIC, University of North Carolina at Chapel Hill, Chapel Hill, NC, USA
gang_li@med.unc.edu

Abstract. The human cerebral cortex develops dynamically during the early postnatal stage, reflecting the underlying rapid changes of cortical microstructures and their connections, which jointly determine the functional principles of cortical regions. Hence, the dynamic cortical developmental patterns are ideal for defining the distinct cortical regions in microstructure and function for neurodevelopmental studies. Moreover, given the remarkable inter-subject variability in terms of cortical structure/function and their developmental patterns, the *individualized* cortical parcellation based on each infant's own developmental patterns is critical for precisely localizing personalized distinct cortical regions and also understanding inter-subject variability. To this end, we propose a novel method for individualized parcellation of the infant cortical surface into distinct and meaningful regions based on each individual's cortical developmental patterns. Specifically, to alleviate the effects of cortical measurement errors and also make the individualized cortical parcellation comparable across subjects, we first create a *population*-based cortical parcellation to capture the general developmental landscape of the cortex in an infant population. Then, this *population*-based parcellation is leveraged to guide the *individualized* parcellation based on each infant's own cortical developmental patterns in an *iterative* manner. At each iteration, the individualized parcellation is gradually updated based on (1) the prior information of the *population*-based parcellation, (2) the *individualized* parcellation at the previous iteration, and also (3) the developmental patterns of all vertices. Experiments on fifteen healthy infants, each with longitudinal MRI scans acquired at six time points (i.e., 1, 3, 6, 9, 12 and 18 months of age), show that our method generates a reliable and meaningful individualized cortical parcellation based on each infant's own developmental patterns.

1 Introduction

The human cerebral cortex develops extremely dynamically during the first two postnatal years, with 42% increase in cortical thickness and 115% expansion in cortical surface area [1, 2]. These dynamic development of cortical attributes indeed indicates the rapid changes of the underlying cortical microstructures and their connections (e.g., increases in dendritic arborization, axonal elongation and thickening, synaptogenesis and glial proliferation), which jointly determine the molecular organization and functional principles of cortical regions [1]. Hence, the developmental patterns of cortical

M. Descoteaux et al. (Eds.): MICCAI 2017, Part I, LNCS 10433, pp. 66–74, 2017.
DOI: 10.1007/978-3-319-66182-7_8

attributes can help better define the microstructurally, functionally and developmentally distinct regions of the cortex than the conventional macro-anatomical sulcal-gyral landmarks, which are extremely variable across individuals and poorly aligned with the microstructural and functional borders [3]. Therefore, parcellation of infant cortical surface into distinct and meaningful regions based on the dynamic cortical developmental patterns is of great importance in neuroimaging mapping of early brain development, e.g., both region-based and network-based analyses.

Given the remarkable inter-subject variability in terms of cortical structure and function [4], as well as their developmental trajectories, each individual is expected to have a unique architecture in parcellation, reflecting its own unique developmental patterns. The *individualized* cortical parcellation based on each infant's own cortical developmental patterns is important due to the following reasons. (1) It is a crucial step for understanding inter-subject variability and their relationship with behavior and cognitive functions. (2) It is highly important to precisely localize distinct regions in the individual level for discovering meaningful biomarkers of neurodevelopmental disorders rooted during early brain development, and also for personalized targeted clinical applications. (3) It can help improve the accuracy of inter-subject cortical surface registration (for establishing inter-subject cortical correspondences) by leveraging the developmental patterns, e.g., developmentally-distinct regions, thus improving the group-level analysis. This is because conventionally the inter-subject cortical registration is performed based on the cortical folding patterns, which are extremely variable across individuals and typically misaligned with the microstructurally and developmentally defined borders [3]. Hence, methods for precise *individualized* parcellation on the individual infant's cortical developmental patterns is desired.

To achieve this, one straightforward solution is to simply group the growth trajectories of all vertices (of an individual's cortical surface) into distinct clusters based on their similarities. However, this will lead to less comparable results across individuals and also very noisy parcellation due to measurement noises in the infant MR images, which typically exhibit extremely low tissue contrast and dynamic appearances [1, 2].

Motivated by these and inspired by the recent advances in the functional connectivity based brain parcellation in individuals [5, 6], in this paper, we propose a novel method for individualized parcellation of the cortical surface of each infant based on its own developmental patterns of cortical attributes. As an example, we employ cortical thickness as a sensitive indicator of cortical microstructural changes [1]. Other cortical attributes, e.g., surface area, cortical folding, and diffusivity, can also be adopted. In our method, a *population*-based cortical parcellation is first created to capture the general developmental landscape of the cortex in a population of infants. Then, this *population*-based parcellation is further used to initialize and guide the cortical parcellation of an individual infant based on its own developmental patterns in an *iterative* manner, thus leading to precise and reliable *individualized* parcellation that is also comparable across subjects. Specifically, at each iteration, the current individualized parcellation is updated based on (1) the prior information of the population-based parcellation, (2) the individualized parcellation at the previous iteration, and also (3) the developmental trajectories of all vertices of this infant, via minimization of an energy function using a

graph cuts method [7]. Experiments on fifteen healthy infants, each with longitudinal multimodal brain MRI scans acquired at six time points, show that our method generates meaningful cortical parcellation for each infant based on its own developmental patterns.

2 Method

As shown in Fig. 1, the proposed method for the individualized cortical parcellation based on an individual infant's developmental patterns is composed of two major steps: (1) deriving the population-based parcellation and the inter-subject variability map of cortical developmental patterns, and (2) iterative individualized parcellation guided by the population-based parcellation. Each step will be detailed below.

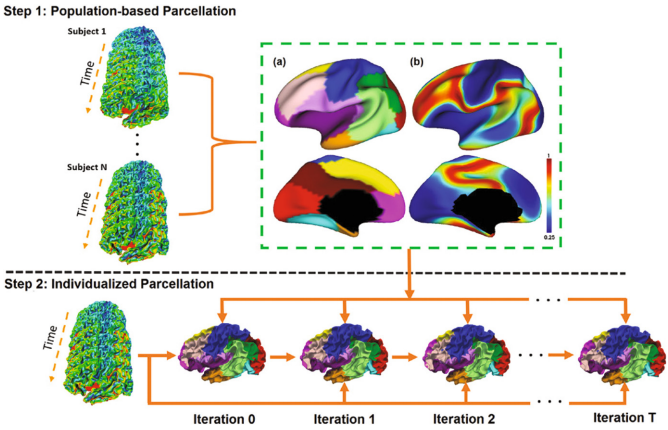

Fig. 1. The proposed method for individualized cortical parcellation based on an infant's cortical developmental patterns. (a) Population-based parcellation and (b) inter-subject variability map, based on the developmental patterns of cortical thickness in a population of infants.

2.1 Population-Based Parcellation and Inter-subject Variability

To derive the population-based parcellation based on the growth patterns of cortical thickness, the spectral clustering method is adopted [8]. Given the developmental trajectories of cortical thickness of all individuals that have been aligned onto the same space, for each infant, its affinity matrix can be first computed by Pearson's correlation of the developmental trajectories of cortical thickness between any pair of vertices on the cortical surface. Then, for each vertex, its inter-subject variability of cortical growth patterns can be estimated as one minus the average of the correlation values between any two subjects' correlation maps at this vertex, as in [4]. Next, the mean affinity matrix of the population is computed as the average of the corresponding elements of affinity matrices of all individual infants. Finally, the spectral clustering is performed on the mean affinity matrix of the population to obtain the population-based cortical

parcellation [9]. As shown in Fig. 1(a), the population-based parcellation using the developmental patterns of cortical thickness leads to a set of spatially-continuous and meaningful regions. Of note, the number of regions is set as 12, to be consistent with both the development-based cortical parcellation [9] and the genetic information-based cortical parcellation [10]. As shown in Fig. 1(b), the inter-subject variability of the growth patterns of cortical thickness is regionally heterogeneous, with low variability in the unimodal cortex as well as insula and anterior medial frontal cortices, but high variability in the high-order association areas (e.g., the lateral prefrontal, inferior parietal, precuneus, and medial temporal cortices).

2.2 Population-Guided Iterative Individualized Parcellation

The population-based parcellation and inter-subject variability map are leveraged to guide the individualized parcellation in an iterative manner, thus gradually leading to precise and reliable individualized parcellations that are comparable across subjects. Specifically, first, the individualized parcellation is initialized by the population-based parcellation (iteration 0), and then is iteratively updated by the minimization of an energy function $E^i = E^i_d + \alpha E^i_s$ at the i-th iteration (Step 2 in Fig. 1). Herein, the weighting parameter α (empirically setting as 10.0) determines the tradeoff between the **data fitting term** E^i_d and the **spatial smoothness term** E^i_s, as detailed below.

Data Fitting Term. The data fitting term is defined based on: (1) the similarity between the developmental trajectory of the vertex x and the representative developmental trajectories of vertices in the region l_x of the individual infant, and (2) the prior spatial information derived from the individualized parcellation at the previous iteration. Letting $P^i_x(l_x)$ be the probability of labeling a vertex x in the individual's cortical surfaces as a region label $l_x \in \{1, \ldots, L\}$, we have:

$$E^i_d = \sum\nolimits_x -\log(P^i_x(l_x)) \tag{1}$$

$$P^i_x(l_x) = \exp\left(\frac{corr(\boldsymbol{s}(x), \boldsymbol{r}^{i-1}(l_x)) - 1}{2}\right) \cdot \frac{\exp(\beta \cdot g^{i-1}_{l_x}(x))}{Z^{i-1}(x)} \tag{2}$$

The **first** component in $P^i_x(l_x)$ is based on the similarity between a vertex's developmental trajectory and a region's *representative trajectory*, and the **second** component is based on the prior shape information of the regions. Herein, $\mathbf{s}(x)$ is the individual's developmental trajectory at the vertex x, and $\boldsymbol{r}^{i-1}(l_x)$ is the *representative trajectory* of the region l_x of the individualized parcellation at the iteration $i-1$; and $corr(\cdot, \cdot)$ represents the Pearson's correlation. Intuitively, a high correlation value indicates a low cost of labeling a vertex x as the region l_x. To incorporate the *guidance* of the population-level parcellation and the subject-specific development, the representative trajectory $\boldsymbol{r}^{i-1}(l_x)$ is computed as a weighted average of two types of trajectories, including: 1) $\boldsymbol{r}_{pop}(l_x)$, which is the average trajectory of *all vertices* in the region l_x defined by the *population*-based parcellation, and 2) $\boldsymbol{r}^{i-1}_{ind}(l_x)$, which is the average trajectory of *reliable vertices* in the region l_x defined by the current

individualized parcellation, thus alleviating the effects of noises and unreliable trajectories. Herein, a vertex is considered reliable if the correlation between this vertex's trajectory and the average trajectory of its assigned region is much larger than its correlation with the average trajectory of any other region in the current individualized parcellation. $\boldsymbol{r}^{i-1}(l_x)$ is computed as: $\boldsymbol{r}^{i-1}(l_x) = \frac{\gamma^i \cdot \boldsymbol{r}_{pop}(l_x) + v^{i-1}(l_x) \cdot \boldsymbol{r}^{i-1}_{ind}(l_x)}{\gamma^i + v^{i-1}(l_x)}$, where $\gamma^i = 1 - i/T$ is a weighting parameter decreasing with the iteration, with T as the total number of iterations, thus gradually reducing the influence of the population-based parcellation during the iterations. And $v^{i-1}(l_x)$ is the average of inter-subject variability map (Fig. 1(b)) in the region l_x, defined by the individualized parcellation at the iteration $i-1$. Intuitively, regions with high inter-subject variability contribute more to the estimation of the core trajectory for the individualized parcellation. In summary, this component encourages labeling a vertex as the region l_x, if they have a high similarity in developmental trajectories.

In the **second** component of P^i_x, $g^{i-1}_{l_x}$ is the *signed* geodesic distance map of the region l_x in the individualized parcellation at the iteration $i-1$, with the inside of the region as positive values. The normalization factor $Z^{i-1}(x)$ is computed as: $Z^{i-1}(x) = \sum_{l=1}^{L} \exp(\beta \cdot g^{i-1}_{l_x}(x))$, with β as a weight parameter setting as 0.04. This formula turns the previous parcellation into spatial probability maps of region labels. Intuitively, vertices close to the region l_x at the previous iteration have high probabilities of being labeled as l_x at the current iteration. Hence, this component encourages to gradually refine the individualized parcellation, thus eliminating abrupt changes that can cause noisy fragments in the parcellation.

Spatial Smoothness Term. This term imposes *adaptive* spatial smoothness into the individualized parcellation. It represents the sum of the costs of labeling of a pair of spatially neighboring vertices on the individual's surfaces:

$$E_s = \sum\nolimits_{\{x,y\} \in \mathcal{N}} V_{x,y}(l_x, l_y) \tag{3}$$

$$V_{x,y}(l_x, l_y) = \exp\left(\frac{corr(\boldsymbol{s}_p(x), \boldsymbol{s}_p(y)) - 1}{2}\right) \times (1 - \delta(l_x - l_y)) \tag{4}$$

Herein, $\mathcal{N}$ is the set of the one-ring neighboring vertex pairs in the subject's cortical surface. $V_{x,y}(l_x, l_y)$ indicates the cost of labeling a pair of spatially neighboring vertices x and y as l_x and l_y. δ is defined as $\delta(l_x - l_y) = 1$ if $l_x = l_y$; otherwise, $\delta(l_x - l_y) = 0$. Intuitively, the neighboring vertices with *similar* developmental trajectories will have a *large* cost, while the neighboring vertices with quite *different* developmental trajectories will have a *small* cost, when assigning different labels to them. Thus, this term adaptively encourages the spatial smoothness in the parcellation, based on the similarity of neighboring vertices' developmental trajectories.

Energy Minimization. To efficiently solve this energy minimization problem, the alpha-expansion graph cuts method is adopted, which can guarantee a strong local minimum for our defined energy function [7].

3 Results

Dataset and Image Processing. To validate the proposed method, we employed a longitudinal dataset including fifteen healthy infants, each with its longitudinal multimodal MRI scans (T1-, T2- and diffusion-weighted imaging) at 6 time points, i.e., 1, 3, 6, 9, 12, and 18 months of age. All MR images were processed by an infant-tailored computational pipeline, which includes the subsequent procedures of skull stripping, intensity inhomogeneity correction, tissue segmentation, hemisphere separation, topology correction, cortical surface reconstruction, cortical thickness smoothing and normalization, and intra-subject/inter-subject surface registration [9, 11].

Validation. To illustrate how the individualized parcellation changes during the iterations, Fig. 2 provides the results from two representative subjects, with the zooming views of two typical regions. As we can see, the individualized parcellation changes gradually, which is obvious especially in the regions with high inter-subject variability of cortical developmental patterns (Fig. 1(b)), e.g., the middle frontal gyrus and supramarginal gyrus. Although there is no ground truth for the individualized parcellation based on developmental patterns, ideally the vertices within the same region should exhibit high correlations of growth trajectories, while vertices across different regions should exhibit low correlations of growth trajectories. Therefore, for each subject, Fig. 3(a) provides the average values of the Pearson's correlations of growth trajectories of any pair of vertices within the same parcellated region at different

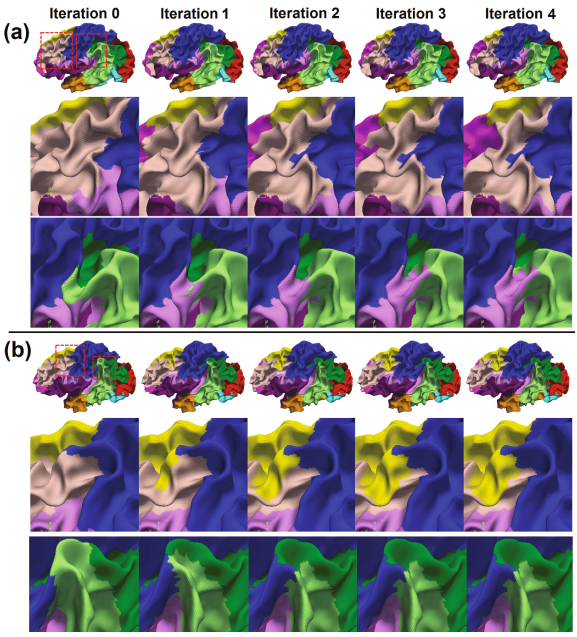

Fig. 2. Illustration of iterative changes of individualized parcellation on two subjects: (a) and (b). The zooming views of two regions enclosed by the red rectangles are also provided.

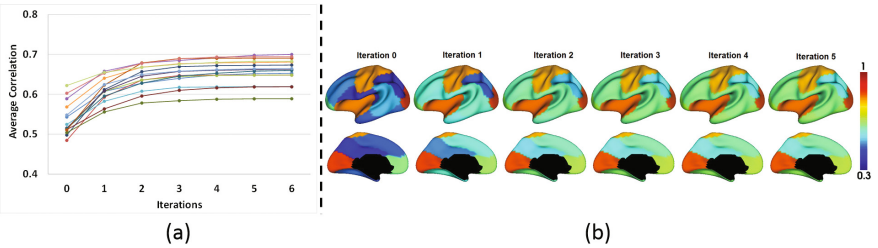

Fig. 3. Illustration of the average within-region correlation of cortical growth patterns during the iterations. (a) The average correlation of all regions for each subject, with each curve indicating one subject. (b) The average correlation of all subjects in each region.

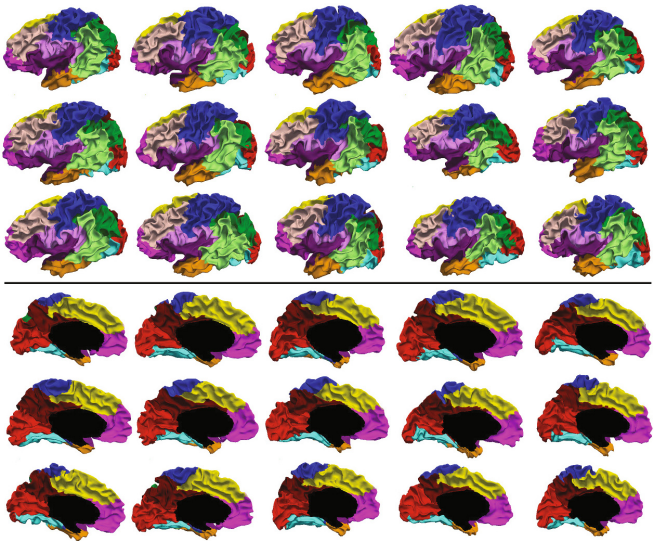

Fig. 4. Results of the individualized cortical parcellation for each of the fifteen infants, based on each individual's own developmental patterns of cortical thickness.

iterations. As we can see, for each subject, the average correlation typically increases dramatically in the first iteration, and then gradually until 5 iterations. For each region, Fig. 3(b) further shows that the average within-region correlations of growth trajectories of all subjects at different iterations, indicating that our method greatly improves the within-region homogeneity of growth patterns, especially in the high-order association areas, e.g., prefrontal, temporal, and parietal cortices. Figure 4 shows the individualized parcellation based on each subject's developmental patterns of cortical thickness for each of the fifteen infants. This renders both the certain commonality and remarkable region-specific variability across subjects in their individualized parcellations, especially in the high-order association areas, e.g., prefrontal and parietal cortices. These results suggest that the inter-subject variability of developmental patterns is

captured by our method. Interestingly, the prefrontal and parietal cortices also showed high inter-subject variability in both the functional connectivity and the individualized functional parcellation as reported in [4, 6], indicating that our results are scientifically meaningful.

4 Conclusion

This paper presented a novel method for individualized parcellation of each infant's cortical surfaces based on its own developmental patterns. By leveraging the guidance from the *population*-based parcellation, our method iteratively generates a reliable *individualized* parcellation that is easily comparable across different subjects. Note that the individualized parcellation could be used to improve the accuracy of inter-subject cortical surface registration, e.g., using the boundaries of regions in the individualized parcellation for guiding surface registration, thus possibly further improving accuracy of *population*-based parcellation, which will be investigated in future.

Acknowledgements. This work was supported in part by NIH grants (MH100217, MH107815, MH108914, MH109773, and MH110274).

References

1. Lyall, A.E., Shi, F., Geng, X., Woolson, S., Li, G., Wang, L., Hamer, R.M., Shen, D., Gilmore, J.H.: Dynamic development of regional cortical thickness and surface area in early childhood. Cereb. Cortex **25**, 2204–2212 (2015)
2. Li, G., Lin, W., Gilmore, J.H., Shen, D.: Spatial patterns, longitudinal development, and hemispheric asymmetries of cortical thickness in infants from birth to 2 years of age. J. Neurosci. **35**, 9150–9162 (2015)
3. Zilles, K., Amunts, K.: Centenary of Brodmann's map—conception and fate. Nat. Rev. Neurosci. **11**, 139–145 (2010)
4. Mueller, S., Wang, D., Fox, M.D., Yeo, B.T., Sepulcre, J., Sabuncu, M.R., Shafee, R., Lu, J., Liu, H.: Individual variability in functional connectivity architecture of the human brain. Neuron **77**, 586–595 (2013)
5. Wang, D., Buckner, R.L., Fox, M.D., Holt, D.J., Holmes, A.J., Stoecklein, S., Langs, G., Pan, R., Qian, T., Li, K.: Parcellating cortical functional networks in individuals. Nat. Neurosci. **18**, 1853–1860 (2015)
6. Laumann, T.O., Gordon, E.M., Adeyemo, B., Snyder, A.Z., Joo, S.J., Chen, M.-Y., Gilmore, A.W., McDermott, K.B., Nelson, S.M., Dosenbach, N.U.: Functional system and areal organization of a highly sampled individual human brain. Neuron **87**, 657–670 (2015)
7. Boykov, Y., Kolmogorov, V.: An experimental comparison of min-cut/max-flow algorithms for energy minimization in vision. IEEE Trans. PAMI **26**, 1124–1137 (2004)
8. Ng, A.Y., Jordan, M.I., Weiss, Y.: On spectral clustering: analysis and an algorithm. Adv. Neural. Inf. Process. Syst. **2**, 849–856 (2002)
9. Li, G., Wang, L., Shi, F., Lin, W., Shen, D.: Constructing 4D infant cortical surface atlases based on dynamic developmental trajectories of the cortex. In: Golland, P., Hata, N., Barillot, C., Hornegger, J., Howe, R. (eds.) MICCAI 2014. LNCS, vol. 8675, pp. 89–96. Springer, Cham (2014). doi:10.1007/978-3-319-10443-0_12

10. Chen, C.-H., Fiecas, M., Gutierrez, E., Panizzon, M.S., Eyler, L.T., Vuoksimaa, E., Thompson, W.K., Fennema-Notestine, C., Hagler, D.J., Jernigan, T.L.: Genetic topography of brain morphology. PNAS **110**, 17089–17094 (2013)
11. Li, G., Wang, L., Shi, F., Lin, W., Shen, D.: Simultaneous and consistent labeling of longitudinal dynamic developing cortical surfaces in infants. Med. Image Anal. **18**, 1274–1289 (2014)